Autophagy of Intestinal Epithelial Cells Inhibits Colorectal Carcinogenesis Induced by Colibactin-Producing Escherichia coli in Apc Mice

Cecily Lucas, Laurène Salesse, My Hanh Thi Hoang, Mathilde Bonnet, Pierre Sauvanet, Anaïs Larabi, Catherine Godfraind, Johan Gagnière, Denis Pezet, Philip Rosenstiel, et al.

Autophagy of Intestinal Epithelial Cells Inhibits Colorectal Carcinogenesis Induced by Colibactin-producing *Escherichia coli* in $Apc^{Min/+}$ Mice

Cécily Lucas[1], Laurène Salesse[1], My Hanh Thi Hoang[1,2], Mathilde Bonnet[1], Pierre Sauvanet[1,3], Anaïs Larabi[1], Catherine Godfraind[1,4], Johan Gagnière[1,3], Denis Pezet[1,3], Philip Rosenstiel[5], Nicolas Barnich[1], Richard Bonnet[1,6], Guillaume Dalmasso[1], Hang Thi Thu Nguyen[1].

[1]M2iSH, UMR 1071 Inserm, University of Clermont Auvergne, INRA USC 2018, CRNH, Clermont-Ferrand 63001, France.

[2]Department of Cell Biology, Faculty of Biology, University of Science, Vietnam National University (VNU), Hanoi, Vietnam.

[3]Department of Digestive and Hepatobiliary Surgery, CHU Clermont-Ferrand, France.

[4]Department of Pathology, CHU Gabriel Montpied, Clermont-Ferrand, France.

[5]Institute of Clinical Molecular Biology, Christian-Albrechts-University and University Hospital Schleswig-Holstein, Kiel, Germany.

[6]Department of Bacteriology, CHU Gabriel Montpied, Clermont-Ferrand, France.

*__Address correspondence to__: Hang Nguyen, PhD. Phone: 33 4 73 17 83 72. Fax: 33 4 73 17 83 71. E-mail: hang.nguyen@uca.fr. Mailing address: M2iSH, UMR 1071 Inserm, University of Clermont Auvergne, 28 Place Henri-Dunant, Clermont-Ferrand 63001, France.

Short Title: Autophagy inhibits colibactin-induced CRC

Grant support: This work was supported by the Ministère de la Recherche et de la Technologie, Inserm (UMR1071) and INRA (USC 2018), the Agence Nationale de la Recherche of the French government through the program ‘‘Investissements d’Avenir’’ (16-IDEX-0001 CAP 20-25) (to H.N.), the European Union FP7 People Marie Curie International Incoming Fellowship (to H.N.) and the DFG ExC Precision Medicine in Chronic Inflammation and the CRC1182 project C2 (to P.R.).

Abbreviations: $Apc^{Min/+}/Atg16l1^{\Delta IEC}$, $Apc^{Min/+}$ mice deficient for *Atg16l1* specifically in intestinal epithelial cells; CFU, colony-forming units; CoPEC, colibactin-producing *Escherichia coli*; CRC, colorectal cancer; DSBs, double-strand breaks; IECs, intestinal epithelial cells; *pks*, polyketide synthase.

Acknowledgement: We would like to thank Prof. Xavier Ramnik (Harvard Medical School, Boston, USA) for kindly providing us CRISPR-Cas9-mediated *ATG16L1* knock-out Hela cells. We thank the platform CLIC (CLermont-ferrand Imagerie Confocale, Université Clermont Auvergne) for assistance with the confocal microscopy.

Author contributions: Cécily Lucas performed the experiments, analyzed and interpreted data. Laurène Salesse, Hanh Hoang, Pierre Sauvanet and Anaïs Larabi performed the experiments. Catherine Godfraind performed histological examination. Johan Gagnière and Denis Pezet were involved in patient inclusion and human sample collection. Philip Rosenstiel supported materials and supervised the manuscript. Guillaume Dalmasso, Mathilde Bonnet, Nicolas Barnich and Richard Bonnet critically revised the manuscript for important intellectual content. Hang Nguyen developed experimental concepts and designs, performed the experiments, analyzed and interpreted data and wrote the manuscript.

The author has nothing to disclose.

Abstract

Background and aims: Colibactin-producing *Escherichia coli* (CoPEC) colonize the colon mucosa of higher proportions of patients with vs without colorectal cancer (CRC) and promote colorectal carcinogenesis in susceptible mouse models of CRC. Autophagy degrades cytoplasmic contents, including intracellular pathogens, via lysosomes and regulates intestinal homeostasis. We investigated whether inhibiting autophagy affects colorectal carcinogenesis in susceptible mice infected with CoPEC.

Methods: Human intestinal epithelial cells (IECs, HCT-116) were infected with a strain of CoPEC (11G5 strain) isolated from a patient or a mutant strain that does not produce colibactin (11G5ΔclbQ). Levels of ATG5, ATG16L1, and SQSTM1 (also called p62) were knocked down in HCT-116 cells using small interfering RNAs. $Apc^{Min/+}$ mice with and without IEC-specific disruption of *Atg16l1* ($Apc^{Min/+}/Atg16l1^{\Delta IEC}$) were infected with 11G5 or 11G5ΔclbQ. Colonic tissues were collected from mice and analyzed for tumor size and number and by histology, immunoblot, and quantitative reverse transcription PCR analyses for markers of autophagy, DNA damage, cell proliferation and inflammation. We analyzed levels of mRNAs encoding proteins involved in autophagy in colonic mucosal tissues from patients with sporadic CRC colonized with vs without CoPEC by quantitative reverse transcription PCR.

Results: Patient colonic mucosa with CoPEC colonization had higher levels of mRNAs encoding proteins involved in autophagy than colonic mucosa without these bacteria. Infection of cultured IECs with 11G5 induced autophagy and DNA damage repair, whereas infection with 11G5ΔclbQ did not. Knockdown of ATG5 in HCT-116 cells increased numbers of intracellular 11G5, secretion of interleukin 6 (IL6) and IL8, and markers of DNA double-strand breaks, but reduced markers of DNA repair, indicating that autophagy is required for bacteria-induced DNA damage repair. Knockdown of ATG5 in HCT-116 cells increased 11G5-induced senescence, promoting proliferation of uninfected cells. $Apc^{Min/+}/Atg16l1^{\Delta IEC}$ mice developed fewer and smaller colon tumors than $Apc^{Min/+}$ mice. However, following infection with 11G5, $Apc^{Min/+}/Atg16l1^{\Delta IEC}$ mice developed more and larger tumors, with a significant increase in mean histologic score, than infected $Apc^{Min/+}$ mice. Increased levels of *Il6*, *Tnf,* and *Cxcl1* mRNAs, and decreased level of *Il10* mRNA, and increased markers of DNA double-strand breaks and proliferation were observed in colonic mucosa of 11G5-infected $Apc^{Min/+}/Atg16l1^{\Delta IEC}$ mice vs 11G5-infected $Apc^{Min/+}$ mice.

Conclusion: Infection of IECs and susceptible mice with CoPEC promotes autophagy, which is required to prevent colorectal tumorigenesis. Loss of ATG16L1 from IECs increases markers of inflammation, DNA damage, and cell proliferation and increases colorectal tumorigenesis in $Apc^{Min/+}$ mice. These findings indicate the importance of autophagy in response to CoPEC infection and strategies to induce autophagy might be developed for patients with CRC and CoPEC colonization.

Keywords: microbiome, pathogenic bacteria, toxin, colon cancer.

Introduction

Colorectal cancer (CRC) is the third most common cancer, affecting about 1.36 million of new cases per year, and is the fourth leading cause of cancer-related death worldwide with 700,000 death per year[1]. CRC is a multifactorial disease, of which several risk factors have been identified, such as age, genetic factors, unhealthy behaviors, microbial factors and inflammatory bowel diseases. Among them, the gut microbiota has been emerged as a key player in CRC development. A modification of gut microbiota composition or dysbiosis has been reported in CRC patients with an increase in *Bacteroides fragilis*, *Streptococcus bovis/gallolyticus*, *Escherichia coli*, *Enterococcus faecalis* and *Fusobacterium nucleatum* and a decrease in *Faecalibacterium prausnitzii*[2]. The involvement of gut microbiota in CRC has been then determined using mouse models of CRC. One of the best-known CRC models is $Apc^{Min/+}$ mice bearing a loss-of-function germinal mutation in the *Apc* gene[3], which is the most prevalent mutation and has been found in about 80% of CRC[4]. Germ-free $Apc^{Min/+}$ mice display lower number of intestinal and colorectal tumors compared to microbiota-bearing $Apc^{Min/+}$ mice[5]. Similar results were obtained for the CRC mouse model chemically induced by azoxymethane (AOM) and dextran sodium sulfate (DSS)[6]. Germ-free mice colonized with the fecal microbiota from AOM-DSS-treated mice exhibit enhanced colorectal tumorigenesis compared to those colonized with the gut microbiota from untreated mice, suggesting that the dysbiotic microbiota directly contributes to colorectal carcinogenesis[6]. A recent study showed that conventional mice treated with antibiotics and then with AOM or germ-free mice receiving fecal samples from CRC patients exhibit increases in polyp numbers, intestinal dysplasia and proliferation, and inflammation, compared with those receiving fecal samples from healthy individuals[7]. These studies provided evidence that a CRC-associated dysbiotic microbiota can promote colorectal carcinogenesis.

Studies have shown a higher prevalence of colonic mucosa-associated *E. coli* in CRC patients compared to control subjects[2]. Particularly, *E. coli* strains harboring the polyketide synthase (*pks*) pathogenicity island, which encodes the genotoxin colibactin, have attracted growing research interest. Colibactin-producing *E. coli*, designated as CoPEC, have been identified in the colonic mucosa of ~55.3% CRC patients vs 19.3% patients with diverticulosis[8]. CoPEC have been shown to induce DNA double-strand breaks (DSBs), chromosomic instability and cell cycle arrest[9,10]. CoPEC also induce senescence of infected cells accompanied by secretion of inflammatory mediators and growth factors, thus promoting proliferation of adjacent uninfected cells[11]. Importantly, CoPEC are able to promote colon tumorigenesis in CRC mouse models, including $Apc^{Min/+}$ mice[12], AOM-treated $il10^{-/-}$ mice[13],

AOM/DSS-treated mice[11] and *Apc*$^{Min/+}$*/il10*$^{-/-}$ mice[14]. CoPEC might therefore promote colorectal carcinogenesis by inducing genomic instability, as well as inducing intestinal cell senescence and inflammation.

Autophagy is a lysosome-dependent degradative process that targets intracellular components, such as damaged organelles, misfolded proteins, toxic aggregates and intracellular pathogens, into double-membraned vesicles known as autophagosomes, which fuse with lysosomes to form autolysosomes, where the cargos are degraded. Autophagy is considered as a major survival mechanism by conferring stress tolerance, limiting damage, and sustaining cellular viability under adverse conditions[15]. Autophagy deficiency causes oxidative stress and genomic instability, and has contributed to the pathogenicity of many diseases including cancers and infectious diseases[15]. In tumorigenesis, autophagy has a complex and dual role. Indeed, some studies have highlighted its anti-tumoral role by protecting cells from conditions contributing to transformation and carcinogenesis such as oxidative stress, DNA damage, genetic instability and inflammation. However, other studies have described a pro-tumoral role of autophagy with its ability to protect cancer cells from metabolic stress and hypoxia in the tumor microenvironment[16].

Recently, several studies have revealed a link between autophagy and CRC. Increased level of LC3-II, the form associated with the autophagosomes, was observed in colorectal tumors compared to normal tissues in CRC patients[17]. A positive correlation between LC3 protein expression and tumor aggressiveness was also reported[17]. Increased expression of the autophagy-related protein ATG10 in CRC was associated with tumor invasion and metastasis[18]. Furthermore, 5-year survival rate of patients bearing tumors without ATG10 expression was significantly higher than patients with ATG10-expressing tumors[18]. Nevertheless, CRC patients with higher expression of the autophagic proteins BECLIN 1, LC3B and BCL-xL both in the center of tumor and adjacent non-cancerous mucosa, compared to those with lower expression, have a better overall survival rate[19]. So far, the role of autophagy in CRC is complex and remains poorly understood.

Here, we investigated the implication of autophagy in host defense to carcinogenic effects of CoPEC strains and in CRC development induced by the latter.

Materials and methods

Information on bacterial strains, CoPEC colonization in CRC patient samples, cell culture, infection and invasion assay, siRNA transfection, protein extraction and Western blot, total RNA extraction, cDNA synthesis, quantitative reverse transcription PCR (qRT-PCR), ELISA, senescence-associated β-galactosidase staining, immunofluorescent microscopy, histological examination, and immunohistochemical staining appears in the **Supplementary information.**

Bacterial strains and culture

The clinical *E. coli* strains isolated from CRC patients[8,20], the K12 C600 strain, the non-pathogenic *E. coli* MG1655 strain, the commensal *E. coli* HS strain, the clinical 11G5 strain and its isogenic mutant 11G5Δ*clbQ* depleted for the *clbQ* gene in the *pks* island and unable to produce colibactin[21] were grown at 37°C in Luria-Bertani (LB) medium overnight.

Animal model and infection of mice

$Apc^{Min/+}$ mice deficient for *Atg16l1* specifically in IECs ($Apc^{Min/+}$/$Atg16l1^{\Delta IEC}$) and their littermate controls ($Apc^{Min/+}$/$Atg16l1^{flox/flox}$, hereafter defined as $Apc^{Min/+}$) were generated using C57BL/6J-$Apc^{Min/+}$ mice (The Jackson Laboratory) and $Atg16l1^{\Delta IEC}$ or $Atg16l1^{flox/flox}$ mice[22]. Mice were infected or not with the 11G5 strain or the mutant 11G5Δ*clbQ* as previously described[12] and sacrificed at day 65 post-infection. Colonic tumor number and tumor volume [(width^2 x length)/2] were determined using a dissecting microscope. The colons were then swiss-rolled and fixed in buffered 10% formalin and embedded in paraffin. Non-tumoral mucosa was frozen at -80°C for protein and RNA extraction.

Ethical statement

Animal protocols were in accordance with the recommendations of the Guide for the care and use of laboratory animals of the Université Clermont Auvergne and were approved by the Ministère de l'Education Nationale, de l'Enseignement Supérieur et de la Recherche (APAFIS#11254).

Samples from CRC patients came from the MiPaCor collection (Ethical approval for human study N°DC-2017-2972). Patients underwent surgery for resectable CRC in the Digestive and Hepatobiliary Surgery Department of the University Hospital of Clermont-Ferrand. All patients were adult volunteers and signed informed consent before inclusion in

the study. The exclusion criteria included clinically suspected hereditary CRC using the revised Bethesda criteria[23], neo-adjuvant chemotherapy, history of previous colonic resection, emergency surgery and use of antibiotics within 4 weeks before surgery. Macroscopically normal mucosa samples adjacent to the tumor (10cm from the tumor) were collected as previously described[12,24].

Statistical analysis

Results are presented as means ± SEM or median. Statistical analyses between two or several groups were performed using Student's t-test (Mann-Whitney if not parametric) or ANOVA followed by a post-test Bonferroni (Kruskal-Wallis if not parametric) respectively with GraphPad Prism. A P value less than .05 was considered statistically significant. *P<.05; **P≤.01; ***P≤.001.

Results

Colonization of non-tumoral colonic mucosa from CRC patients with CoPEC is associated with high mRNA expression levels of autophagy-related genes.

To investigate the potential link between autophagy and CoPEC colonization, we analyzed mRNA levels of different autophagy genes by qRT-PCR in the normal colonic mucosa from patients with sporadic CRC colonized with CoPEC or with *E. coli* strains that do not carry the *pks* island, designated as *E. coli/pks-* **(Figures 1A and S1)**. A significant increase in mRNA expression levels of several autophagy-related genes was observed in the mucosa colonized with CoPEC compared to those colonized with *E. coli/pks-* (**Figure 1A**). The proportion of patients with high mRNA levels of autophagy-related genes (> median) was increased in the group having CoPEC colonization compared to the *E. coli/pks-* group (**Figure 1B**). These data suggest that CoPEC colonization in the CRC mucosa is associated with autophagy activation.

CoPEC infection induces autophagy in human colon cancer cells, and this requires the *pks* island.

To support the data using patient samples, human CRC cells HCT-116 were infected with the clinical CoPEC 11G5 strain or its mutant 11G5*ΔclbQ* unable to produce colibactin[21] or the transcomplemented 11G5 strain, and levels of mRNAs encoding proteins involved in autophagy were assessed. **Figure S2** shows that infection with 11G5 or the transcomplemented 11G5 strain increased mRNA levels of several genes implicated in autophagy process compared to 11G5*ΔclbQ* infection.

We next investigated whether autophagy is activated in HCT-116 cells following infection with different clinical CoPEC strains[8,20] by analyzing the levels of LC3-I (cytosolic form) and LC3-II (autophagosome-associated form) by Western blot. Infection with CoPEC strains resulted in increased LC3-II level, indicating autophagy activation, compared to uninfected condition or infection with the non-pathogenic *E. coli* K12 C600 or MG1655 strains, or with the commensal *E. coli* HS strain or the clinical *E. coli/pks-* strains (**Figure 1C, D**). Induction of a degradative autophagy in CoPEC-infected HCT-116 cells was confirmed by the concomitant decrease in SQSTM1 (also called p62), a receptor protein degraded by functional autophagy (**Figure 1C, D**). These were not observed with *E. coli/pks-* infection (**Figure 1C, D**), suggesting that autophagy is specifically activated upon CoPEC infection.

To confirm the implication of the *pks* island in autophagy activation, HCT-116 cells were infected with the 11G5 strain or its mutant 11G5Δ*clbQ*. As expected, 11G5 infection led to autophagy activation, as evidenced by increased LC3-II level and SQSTM1 degradation. This was not observed following 11G5Δ*clbQ* infection (**Figure 1E, F**). Infection with the transcomplemented 11G5 strain resulted in similar results as obtained for 11G5 infection (data not shown). Furthermore, the increase in LC3-II level induced by 11G5 infection was also observed in cells treated with the inhibitor of autophagy flux bafilomycin A1, indicating that 11G5 infection induces autophagy rather than blocks autophagy flux (**Figure S3**).

Autophagy is necessary to eliminate intracellular 11G5 bacteria and inhibit 11G5-induced inflammation.

As autophagy is a key process to eliminate intracellular bacteria, we sought to check intracellular 11G5 number and pro-inflammatory cytokine production in autophagy-defective cells. We inhibited autophagy by transfecting HCT-116 cells with *ATG5*-specific siRNA, which markedly reduced ATG5 protein expression compared to scramble siRNA **(Figure S4)**. An increase in intracellular 11G5 number was observed in *ATG5* siRNA-transfected compared to scramble siRNA-transfected cells **(Figure 1G)**. Secreted IL6 and IL8 levels were increased following 11G5 infection in scramble siRNA-transfected cells, and this increase was more pronounced in *ATG5* siRNA-transfected cells **(Figure 1H)**. Similarly, *ATG16L1* siRNA-transfected cells exhibited increases in intracellular 11G5 number and secreted IL6 and IL8 levels compared to scramble siRNA-transfected cells **(Figure S5)**. These data indicate that ATG5- and ATG16L1-dependent autophagy is necessary to eliminate intracellular 11G5 bacteria and to inhibit 11G5-induced inflammation.

Autophagy is necessary for DNA damage repair following CoPEC infection.

In cells transfected with vehicle or scramble siRNA, the level of γH2AX, a marker of DNA DSBs, was increased upon 11G5 infection compared to that in uninfected cells or in cells infected with the MG1655 strain or the 11G5Δ*clbQ* mutant **(Figure 2A, B)**. Following 11G5 infection, γH2AX level was markedly increased in *ATG5* siRNA-transfected vs scramble siRNA-transfected cells (**Figure 2A, B**). These results were confirmed using Hela cells, in which *ATG16L1* gene was depleted by the CRISPR-Cas9 gene editing system **(Figure S6)**. Immunofluorescent labeling of γH2AX consistently showed an accumulation of γH2AX foci, indicating phosphorylation of histone H2AX at the site of DNA DSBs,

following 11G5 infection in both *ATG5* siRNA-transfected and scramble siRNA-transfected HCT-116 cells. Furthermore, this accumulation was more important in *ATG5* siRNA-transfected cells (**Figure 2C, D**).

Next, we analyzed the recruitment of RAD51 into the nucleus, which plays a central role in DNA damage repair. Following 11G5 infection, Western blot analysis showed increased RAD51 level in the nuclear fraction from scramble siRNA-transfected cells, indicating DNA repair activation, and this was inhibited in *ATG5* siRNA-transfected cells (**Figure 2E, F**). As accumulation of SQSTM1 in cells with defective autophagy was shown to inhibit the recruitment of DNA repair proteins, such as RAD51, to the sites of DNA DSBs, thus impairing DNA damage repair[25], we investigated whether the observed effects were SQSTM1-dependent. As expected, SQSTM1 was accumulated in the nuclear fraction from *ATG5* siRNA-transfected cells compared to scramble siRNA-transfected cells (**Figure 2E, F**). However, in cells transfected with both *ATG5* siRNA and *SQSTM1* siRNA, SQSTM1 level was markedly decreased **(Figure 2E, F).** Importantly, *SQSTM1* siRNA abolished the inhibition of RAD51 recruitment into the nucleus upon 11G5 infection in *ATG5* siRNA-transfected cells, as we observed RAD51 recruitment into the nucleus in cells transfected with both *ATG5* and *SQSTM1* siRNAs to a similar level with that in scramble siRNA-transfected cells (**Figure 2E, F**). This showed that SQSTM1 accumulation in autophagy-deficient cells is responsible for the inhibition of DNA damage repair. Immunofluorescent staining consistently showed an accumulation of RAD51 foci in the nucleus and at the nuclear periphery in scramble siRNA-transfected cells upon 11G5 infection, and this was blocked in *ATG5* siRNA-transfected cells (**Figure 2G, H**). However, inhibition of SQSTM1 expression in *ATG5* siRNA-transfected cells increased RAD51 foci number upon 11G5 infection to a level similar to what was observed in scramble siRNA-transfected cells (**Figure 2G, H**). Together, these results show that upon CoPEC infection, a functional autophagy is necessary to activate DNA damage repair, and this is dependent on SQSTM1.

Autophagy deficiency leads to enhanced CoPEC-induced cellular senescence, promoting proliferation of uninfected cells.

To investigate the role of autophagy in CoPEC-induced cellular senescence, we infected HCT-116 cells pre-transfected with scramble or *ATG5* siRNA with 11G5 or 11G5Δ*clbQ*, and detected senescent cells by β-galactosidase staining at pH 6. 11G5 infection increased the number of β-galactosidase-positive cells in scramble siRNA-transfected cells, and this

number was markedly increased in *ATG5* siRNA-transfected cells (**Figure S7A, B**). These results were confirmed using *ATG16L1*-knock out Hela cells (**Figure S8**).

Conditioned media derived from cells transfected with *ATG5* siRNA and infected with 11G5 enhanced HCT-116 cell proliferation compared to that derived from cells transfected with scramble siRNA and infected with 11G5 **(Figure S7C)**. Similar result was not observed for infection with the MG1655 strain or the 11G5Δ*clbQ* mutant. These data show that autophagy deficiency enhances CoPEC-induced cellular senescence, which consequently increases proliferation of uninfected cells.

Together, these data showed that autophagy is activated in IECs upon CoPEC infection, and this is required to limit the inflammatory and carcinogenic effects of the bacteria.

IEC-specific autophagy deficiency increases 11G5-induced colorectal carcinogenesis in *Apc*$^{Min/+}$ mice.

To study the role of autophagy in host susceptibility to CoPEC infection, *Apc*$^{Min/+}$*/Atg16l1*$^{\Delta IEC}$ and *Apc*$^{Min/+}$ mice were orally administered with PBS (uninfected) or with 11G5 or 11G5Δ*clbQ* bacteria. Under uninfected or 11G5Δ*clbQ*-infected conditions, *Apc*$^{Min/+}$*/Atg16l1*$^{\Delta IEC}$ mice exhibited increased body weight compared to *Apc*$^{Min/+}$ mice since day 44 or day 36 post-administration respectively **(Figure 3A)**. Uninfected *Apc*$^{Min/+}$*/Atg16l1*$^{\Delta IEC}$ mice exhibited increased body weight, and this could be explained by the fact that these mice were in good health and showed no pale feet or rectal prolapse. This was consistent with the study by Lévy *et al.*, which reported that *Apc*$^{Min/+}$ mice following tamoxifen-mediated *Atg7* inactivation specifically in IECs showed no signs of illness, and the occurrence of intestinal neoplasia was very rare[26]. In contrast, following 11G5 infection, a decrease in body weight in *Apc*$^{Min/+}$*/Atg16l1*$^{\Delta IEC}$ vs *Apc*$^{Min/+}$ mice was observed since day 44 post-administration **(Figure 3A)**. Furthermore, 11G5-infected *Apc*$^{Min/+}$*/Atg16l1*$^{\Delta IEC}$ mice exhibited decreased body weight compared to uninfected or 11G5Δ*clbQ*-infected *Apc*$^{Min/+}$*/Atg16l1*$^{\Delta IEC}$ mice since day 22 post-administration **(Figure 3A)**.

Shortening of the colon, a macroscopic parameter of tumor development, was more pronounced (*P = .036) in *Apc*$^{Min/+}$*/Atg16l1*$^{\Delta IEC}$ mice (colon length = 6.8 ± 0.28 cm, N = 11) compared to *Apc*$^{Min/+}$ mice (7.58 ± 0.59 cm, N = 13) following 11G5 infection. The representative photos of the colons of each group were shown in **Figure 3B**.

Under uninfected or 11G5Δ*clbQ*-infected conditions, *Apc*$^{Min/+}$*/Atg16l1*$^{\Delta IEC}$ mice had lower number of tumors and decreased tumor volume compared to *Apc*$^{Min/+}$ mice **(Figure 3C,**

D). The decrease in tumorigenesis in *Apc*$^{Min/+}$*/Atg16l1*$^{\Delta IEC}$ mice, which was in consistent with the study by Lévy *et al.*[26], also explained the increase in their body weight compared to *Apc*$^{Min/+}$ mice. However, following 11G5 infection, increases in number and volume of tumors were observed in *Apc*$^{Min/+}$*/Atg16l1*$^{\Delta IEC}$ vs *Apc*$^{Min/+}$ mice **(Figure 3C, D)**. Histological examination consistently showed larger adenocarcinomas with increased inflammatory cell infiltration in the tumors in *Apc*$^{Min/+}$*/Atg16l1*$^{\Delta IEC}$ vs *Apc*$^{Min/+}$ mice following 11G5 infection **(Figure 3E)**. Under uninfected or 11G5Δ*clbQ*-infected conditions, this trend was reversed since compared to *Apc*$^{Min/+}$ mice, *Apc*$^{Min/+}$*/Atg16l1*$^{\Delta IEC}$ mice exhibited less and smaller adenocarcinomas **(Figure 3E)**. Importantly, IEC-specific autophagy deficiency was associated with increased histological score of colonic adenocarcinomas in 11G5-infected *Apc*$^{Min/+}$ mice [16.22 ± 1.623 for *Apc*$^{Min/+}$+11G5 vs 25.43 ± 2.785 for *Apc*$^{Min/+}$*/Atg16l1*$^{\Delta IEC}$+11G5; ***P* = .0093, unpaired *t* test).

Autophagy is necessary to limit 11G5-induced colonic inflammation in *Apc*$^{Min/+}$ mice.

We next investigated the mechanisms by which autophagy limits 11G5-induced colorectal carcinogenesis in *Apc*$^{Min/+}$ mice. Under uninfected condition, mRNA expression levels of the pro-inflammatory cytokines *Il6* and *Tnf* and the chemokine *Cxcl1* were significantly decreased, while that of the anti-inflammatory cytokine *Il10* was increased, in the non-tumoral colonic mucosa of *Apc*$^{Min/+}$*/Atg16l1*$^{\Delta IEC}$ vs *Apc*$^{Min/+}$ mice **(Figure 4)**. In contrast, following 11G5 infection, *Il6*, *Tnf* and *Cxcl1* mRNA levels were increased, whereas *Il10* mRNA level was decreased in the mucosa of *Apc*$^{Min/+}$*/Atg16l1*$^{\Delta IEC}$ vs *Apc*$^{Min/+}$ mice **(Figure 4)**. These results suggest that autophagy limits 11G5-induced colonic inflammation in *Apc*$^{Min/+}$ mice.

Autophagy is necessary to limit 11G5-induced colonic DNA damage in *Apc*$^{Min/+}$ mice.

Next, we verified if a functional autophagy is required to inhibit 11G5-induced DNA damage in *Apc*$^{Min/+}$ mice. First, we examined autophagy activation in the colonic mucosa of mice by Western blot. In uninfected *Apc*$^{Min/+}$ mice, a low level of LC3-II showing basal autophagy activity was observed **(Figure 5A, B)**. This level was increased in the colonic mucosa of 11G5-infected *Apc*$^{Min/+}$ mice **(Figure 5A, B)**, confirming the data on activation of autophagy in IECs upon infection with the CoPEC strains. As expected, we did not detect LC3-II in *Apc*$^{Min/+}$*/Atg16l1*$^{\Delta IEC}$ mice under both uninfected and 11G5 infected conditions **(Figure 5A, B)**.

Western blot analysis showed that γH2AX levels in the non-tumoral colonic mucosa of uninfected groups were not different **(Figure 5C, D)**. 11G5 infection increased γH2AX levels in the colonic mucosa of *Apc*$^{Min/+}$ mice, confirming the data obtained using human IECs. Importantly, the γH2AX levels were increased in 11G5-infected *Apc*$^{Min/+}$*/Atg16l1*$^{\Delta IEC}$ vs 11G5-infeced *Apc*$^{Min/+}$ mice **(Figure 5C, D)**. These results were confirmed by immunohistochemical staining for γH2AX of the colonic sections. **Figure 5E and F** show an increase in the number of γH2AX foci per crypt in the colonic mucosa of *Apc*$^{Min/+}$ mice upon 11G5 infection, and this number was higher in 11G5-infected *Apc*$^{Min/+}$*/Atg16l1*$^{\Delta IEC}$ vs 11G5-infected *Apc*$^{Min/+}$ mice. These results suggest that autophagy is necessary to limit 11G5-induced DNA damage in the colon of *Apc*$^{Min/+}$ mice.

IEC-specific autophagy deficiency leads to increased colonic cell proliferation in 11G5-infected *Apc*$^{Min/+}$ mice.

Finally, the effect of IEC-specific autophagy deficiency on cell proliferation was examined by analyzing the level of Cyclin D1, which is involved in regulating cell cycle progression. Western blot and qRT-PCR analyses consistently showed that Cyclin D1 expression in colonic mucosa was not different between uninfected *Apc*$^{Min/+}$*/Atg16l1*$^{\Delta IEC}$ and *Apc*$^{Min/+}$ mice **(Figure 6A-C)**. 11G5 infection increased Cyclin D1 mRNA and protein expression in the colonic mucosa of *Apc*$^{Min/+}$ mice **(Figure 6A-C)**. Importantly, IEC-specific autophagy deficiency led to increased Cyclin D1 expression in 11G5-infected *Apc*$^{Min/+}$ mice **(Figure 6A-C)**. These results were confirmed by immunohistochemical staining of Ki67, a marker of cell proliferation. The number of Ki67-positive cells in the non-tumoral colonic mucosa was not different between uninfected mice, but following 11G5 infection, this was increased in *Apc*$^{Min/+}$*/Atg16l1*$^{\Delta IEC}$ vs *Apc*$^{Min/+}$ mice **(Figure 6D, E)**. Importantly, the proliferation of tumor cells was also increased in *Apc*$^{Min/+}$*/Atg16l1*$^{\Delta IEC}$ mice compared to *Apc*$^{Min/+}$ mice following 11G5 infection, although this was not different between uninfected groups **(Figure 6F, G)**.

Together, these results show that autophagy deficiency leads to increased proliferation of colonic epithelial cells during 11G5 infection in *Apc*$^{Min/+}$ mice, which could contribute to the development of tumorigenesis.

Discussion

Autophagy has a complex and context-dependent role in carcinogenesis. Autophagy serves as a surveillance mechanism that protects normal cells from the transformation to malignancy by removing damaged organelles and aggregated proteins, and by reducing damaged mitochondria, reactive oxygen species and DNA damage[16]. In addition, autophagy has a crucial role in both innate and adaptive immune responses, thus preventing the establishment and proliferation of malignant cells[27]. Reversely, increasing evidence shows that autophagy can promote tumorigenesis by supporting survival and growth of tumor cells under metabolic and hypoxic stress in the tumor microenvironment, by inhibiting cellular death and increasing anticancer drug resistance[16]. However, a role for autophagy in host responses to infection with CoPEC strains, which have been emerged as an important player in CRC[2], has not yet been investigated.

Here, we showed for the first time the link between autophagy and CoPEC colonization in CRC. Indeed, the colonization of the colonic mucosa from CRC patients with CoPEC is associated with higher expression of several autophagy-associated genes. Modification of autophagy-associated protein expression in CRC has been reported, although the results from different works are inconsistent. Increased expression of autophagy-associated proteins has been shown in most CRC patients and CRC cell lines[17–19,28–30]. However, downregulation of the autophagic protein BECLIN 1 and impairment of autophagy was reported in a small population of CRC[31]. Together with these studies, our data indicate the importance of autophagy in CRC and in particular in CRC with abnormal CoPEC colonization.

We also showed that in HCT-116 colon carcinoma cells, CoPEC infection activates autophagy, and this is dependent on the *pks* island. Previous studies have shown autophagy activation in IECs upon infection with adherent-invasive *E. coli* strains, which abnormally colonize the ileal mucosa of patients with Crohn disease[32–35]. Regarding the link between autophagy and CRC-associated bacteria, it is only beginning to be explored. To date, only two studies are available on the link between autophagy and *Fusobacterium nucleatum*, a CRC-associated bacterium that increases tumor development in $Apc^{Min/+}$ mice[36] and its abundance is correlated with decreased survival rate of CRC patients[37]. *F. nucleatum* infection was reported to activate autophagy, inducing resistance of culture cells to chemotherapeutic drugs[38]. In contrast, Tang *et al.* showed that *F. nucleatum* blocks the autophagic process at the autophagosome-lysosome fusion stage, and this promotes the pro-inflammatory response in the human Caco-2 CRC cell line[39]. Our study therefore contributes to a better understanding of the role of autophagy in the infectious etiology of CRC, an area that is still little explored.

The *pks* island encodes enzymes necessary for the synthesis of colibactin, which has been shown to induce DNA DSBs in mammalian cell lines[10] and in mouse enterocytes[9]. Here, we reported that autophagy is required for DNA damage repair upon infection with the CoPEC 11G5 strain by recruiting the DNA repair protein RAD51 into the nucleus. Our data are consistent with a previous study showing that DNA repair proteins including RAD51 cannot be recruited to the sites of DNA DSBs in autophagy-deficient cells, leading to impaired DNA damage repair[25]. Furthermore, we showed that the autophagy-mediated DNA damage repair is dependent on SQSTM1, a receptor that targets ubiquitinated cargos for degradation via both autophagy and proteasomal pathways[40]. The role of SQSTM1 and autophagy in DNA damage response has been shown. DNA damage and oxidative stress resulting from autophagy defects are suppressed by inhibiting SQSTM1 accumulation[41]. SQSTM1 accumulated in autophagy-defective cells directly binds to and inhibits nuclear RNF168, an E3 ligase essential for histone H2A ubiquitination and DNA damage responses[25]. This consequently inhibits the recruitment of DNA repair proteins, including RAD51, to the sites of DNA DSBs, impairing DNA damage repair[25].

It has been shown that multiple DNA damage induced by CoPEC causes cell cycle arrest and senescence of infected cells[11]. The latter then acquires a senescence-associated secretory phenotype, which is accompanied with the secretion of growth factors that can stimulate uninfected cell proliferation[11]. Here, we showed that autophagy inhibition in HCT-116 cells leads to increased 11G5-induced senescence, which consequently promotes proliferation of uninfected cells. Furthermore, our group showed that CoPEC strains are able to adhere to and to invade IECs, although with a lower level compared to Crohn disease-associated adherent-invasive *E. coli*[21], inducing a pro-inflammatory response[11,21]. Here, we showed that autophagy deficiency in IECs leads to increased 11G5 intracellular replication and enhanced pro-inflammatory cytokine secretion. Together, our data suggest that upon CoPEC infection, autophagy is activated in IECs, and this is important to inhibit the inflammatory and carcinogenic effects of CoPEC strains.

It has been shown that CoPEC induce tumorigenesis in mouse models of CRC[11–14]. However, to date, no data is available on the role of autophagy in CoPEC-induced colorectal carcinogenesis. To study this, we used $Apc^{Min/+}$ mice having IEC-specific autophagy deficiency. $Apc^{Min/+}$ mice are a relevant preclinical tumor model of CRC as mutations in the *APC* gene have been found in more than 80% of sporadic CRC[4]. First, we showed autophagy activation in the colonic mucosa of $Apc^{Min/+}$ mice upon 11G5 infection, which is in consistence with the data using human biopsies and cultured IECs. Furthermore, our work

shed light on the complex role of autophagy in colorectal carcinogenesis in *Apc*$^{Min/+}$ mice. Indeed, without infection, the number and size of colorectal tumors were decreased in *Apc*$^{Min/+}$*/Atg16l1*$^{\Delta IEC}$ vs *Apc*$^{Min/+}$ mice. This was accompanied with decreased pro-inflammatory cytokine mRNA levels and increased anti-inflammatory cytokine mRNA levels in the normal colonic mucosa. These results are in agreement with the study by Lévy *et al.* showing that conditional inactivation of *Atg7* in IECs prevents tumor development in *Apc*$^{Min/+}$ mice via increasing anti-tumor inflammatory responses and affecting tumor cell proliferation[26]. In contrast, following infection with 11G5, *Apc*$^{Min/+}$*/Atg16l1*$^{\Delta IEC}$ mice exhibited increased colonic tumor number and size compared to *Apc*$^{Min/+}$ mice. This can be explained by increased DNA damage, higher pro-inflammatory cytokine and chemokine production in normal colonic mucosa and enhanced cellular proliferation in both normal mucosa and tumors observed for 11G5-infected *Apc*$^{Min/+}$*/Atg16l1*$^{\Delta IEC}$ vs 11G5-infected *Apc*$^{Min/+}$ mice. Importantly, the effect of autophagy on inhibiting colorectal carcinogenesis was specific to infection with colibactin-producing CoPEC strain, since the same effects were not observed for infection with the mutant 11G5Δ*clbQ* unable to produce colibactin.

In conclusion, our work explored a novel role of autophagy as a host defense mechanism against CoPEC colonization in CRC. In particular, we showed for the first time (i) the association between colonization of CoPEC in CRC patients and increased mRNA expression levels of autophagy-related genes and (ii) the molecular mechanism by which autophagy inhibits the pro-tumoral effects of CoPEC and CoPEC-induced colorectal carcinogenesis in *Apc*$^{Min/+}$ mice. Our work also highlighted the complex role of autophagy in colorectal carcinogenesis, since inhibition of autophagy in IECs suppresses colonic tumorigenesis in *Apc*$^{Min/+}$ mice in normal condition, but promotes colorectal carcinogenesis under CoPEC infection condition **(Figure 7)**. This study helps to understand better the mechanism underlying the interaction between the host and CRC-associated CoPEC strains. In the future, this work could contribute to the development of a personalized therapeutic strategy based on autophagy modulation for patients with abnormal CoPEC colonization.

Figure legends

Figure 1: Colonization of the colonic mucosa from CRC patients with CoPEC is associated with high autophagy-related gene expression. Autophagy is activated in human CRC cells upon CoPEC infection to eliminate intracellular bacteria and inhibit inflammation.

(A) qRT-PCR analysis for mRNA expression levels of autophagy-related genes in the normal colonic mucosa from CRC patients colonized with *E. coli/pks*- (34 patients) or CoPEC (31 patients) strains. Each dot in the graphs shows the value for each patient, line at median. Statistical analysis was performed using non-parametric Mann-Whitney test. **(B)** For each autophagy-related gene, the median of mRNA levels of all patients (65 patients) was determined, and the proportion of patients with mRNA levels higher or lower the median was determined. Statistical analysis was performed using Fisher's exact test. $*P < .05$; $**P \leq .01$; $***P \leq .001$. **(C, D)** HCT-116 cells were uninfected or infected with non-pathogenic *E. coli* strains (MG1655, commensal HS or K12 C600) or with clinical *E. coli/pks*- and CoPEC strains. **(E, F)** HCT-116 cells were uninfected or infected with 11G5 or the mutant 11G5Δ*clbQ*. Representative Western blot analysis at 8h post-infection **(C)** or at the indicated time points post-infection **(E).** Quantification of band intensity from 3 independent blots, n = 3/condition **(D, F)**. **(G, H)** HCT-116 cells were transfected with a scramble siRNA or *ATG5* siRNA, and then infected or not with 11G5. **(G)** Intracellular 11G5 number counted on LB agar plates (n = 6/condition). **(H)** Secreted IL6 and IL8 amounts in cell culture supernatant quantified by ELISA (n = 6/condition). **(D, F-H)** Values represent means ± SEM. Statistical analysis was performed using one-way Anova test followed by Bonferroni post-test. $*P < .05$; $**P \leq .01$; $***P \leq .001$; ($^{a'}P < .05$; $^{a}P \leq .001$) *vs* scramble siRNA+11G5 at 0h; $^{b}P \leq .001$ *vs* *ATG5* siRNA+11G5 at 0h.

Figure 2: Autophagy is necessary to limit 11G5-induced DNA damage.

HCT-116 cells were transfected with a scramble or *ATG5* siRNA, or with both *ATG5* siRNA and *SQSTM1* siRNA, and then infected or not with the MG1655 strain, the 11G5 strain or the mutant 11G5Δ*clbQ*. **(A)** Representative Western blot analysis at day 5 post-infection using total cell lysate and **(B)** quantification of band intensity from 3 independent blots. **(C)** Immunofluorescent labeling of γH2AX (red). Nuclei were stained with Hoechst (blue). **(D)** Quantification of γH2AX foci number/nucleus determined from 20 cells/condition and 2 independent experiments. **(E)** Representative Western blot analysis using nuclear fraction

lysate and **(F)** quantification of band intensity from 3 independent blots. **(G)** Immunofluorescent labeling of RAD51 (red). Nuclei were stained with Hoechst (blue). **(H)** Quantification of RAD51 foci number/nucleus determined from 20 cells/condition and 2 independent experiments. Values represent means ± SEM. Statistical analysis was performed using one-way Anova test followed by Bonferroni post-test. *$P < .05$; **$P \leq .01$; ***$P \leq .001$; ($^{a}P \leq .001$; $^{a*}P \leq .01$) *vs* scramble siRNA+11G5; $^{b}P \leq .001$ *vs ATG5* siRNA+*SQSTM1* siRNA+11G5; $^{c}P \leq .001$ *vs ATG5* siRNA uninfected; $^{d}P \leq .001$ *vs ATG5* siRNA+11G5.

Figure 3: IEC-specific autophagy deficiency in *Apc$^{Min/+}$* mice leads to increased 11G5-induced colorectal carcinogenesis.

Apc$^{Min/+}$/Atg16l1$^{\Delta IEC}$ and *Apc$^{Min/+}$* mice were treated with streptomycin for 3 days (day -4), then received H_2O (day -1) for 24h. Mice were orally administered (day 0) with PBS or with 10^9 CFU of 11G5 or 11G5Δ*clbQ* bacteria and sacrificed at day 65 post-administration. **(A)** Body weight of each mouse at different time points was determined, and presented as percentage of body weight of the same mouse at day -4, defined as 100%. Data are means ± SEM. ($^{a}P < .05$; $^{aa}P \leq .01$): *Apc$^{Min/+}$*+PBS *vs Apc$^{Min/+}$/Atg16l1$^{\Delta IEC}$*+PBS. ($^{b}P < .05$; $^{bb}P \leq .01$; $^{bbb}P \leq .001$): *Apc$^{Min/+}$/Atg16l1$^{\Delta IEC}$*+PBS *vs Apc$^{Min/+}$/Atg16l1$^{\Delta IEC}$*+11G5. ($^{c}P < .05$, $^{cc}P \leq .01$): *Apc$^{Min/+}$*+11G5 *vs Apc$^{Min/+}$/Atg16l1$^{\Delta IEC}$*+11G5. ($^{dd}P \leq .01$; $^{ddd}P \leq .001$): *Apc$^{Min/+}$*+11G5Δ*clbQ vs Apc$^{Min/+}$/Atg16l1$^{\Delta IEC}$*+11G5Δ*clbQ*. $^{e}P < .05$: *Apc$^{Min/+}$*+PBS *vs Apc$^{Min/+}$*+11G5. $^{f}P \leq .01$: *Apc$^{Min/+}$*+11G5Δ*clbQ vs Apc$^{Min/+}$*+11G5. (*$P < .05$; **$P \leq .01$; ***$P \leq .001$): *Apc$^{Min/+}$/Atg16l1$^{\Delta IEC}$*+11G5Δ*clbQ vs Apc$^{Min/+}$/Atg16l1$^{\Delta IEC}$*+11G5. **(B)** Representative photos of the colons taken at day of sacrifice. **(C)** The number of colorectal tumors determined using a dissecting microscope. **(D)** Tumor volume (volume of all tumors/number of tumors of each mouse). Data are means ± SEM (uninfected mice: N = 7/group; 11G5Δ*clbQ*-infected mice: N = 8/group; *Apc$^{Min/+}$*+11G5: N = 13; *Apc$^{Min/+}$/Atg16l1$^{\Delta IEC}$*+11G5: N = 11) and are representatives of 2 independent experiments. Statistical analysis was performed using one-way Anova test followed by Bonferroni post-test. *$P < .05$; **$P \leq .01$; ***$P \leq .001$. **(E)** Histological examination using H&E-stained mouse colonic sections. Stars show colorectal tumor; arrowheads show infiltration of immune cells within tumors; arrows show superficial ulcerations in the tumor.

Figure 4: Autophagy is necessary to limit 11G5-induced colonic inflammation in *Apc$^{Min/+}$* mice.

Apc$^{Min/+}$/Atg16l1$^{\Delta IEC}$ and *Apc$^{Min/+}$* mice were orally administered with PBS or with 10^9 CFU of 11G5 bacteria and sacrificed at day 65 post-administration. *Il6*, *Tnf*, *Cxcl1* and *Il10* mRNA levels in the colonic mucosa were quantified by qRT-PCR. Data are means ± SEM (uninfected mice: N = 7/group; *Apc$^{Min/+}$*+11G5: N = 13; *Apc$^{Min/+}$/Atg16l1$^{\Delta IEC}$*+11G5: N = 11) and are representatives of 2 independent experiments. Statistical analysis was performed using one-way Anova test followed by Bonferroni post-test. **P* < .05; ***P* ≤ .01; ****P* ≤ .001.

Figure 5: Autophagy is necessary to limit 11G5-induced DNA damage in the colon in *Apc$^{Min/+}$* mice.

Apc$^{Min/+}$/Atg16l1$^{\Delta IEC}$ and *Apc$^{Min/+}$* mice were orally administered with PBS or with 10^9 CFU of 11G5 bacteria and sacrificed at day 65 post-administration. Representative Western blot analysis of LC3 **(A)** and γH2AX **(C)** levels in the non-tumoral colonic mucosa. **(B, D)** Quantification of band intensity from N = 7/group for uninfected mice and N = 10/group for infected mice. **(E)** γH2AX immunohistochemical staining of non-tumoral colonic mucosa and **(F)** quantification of γH2AX foci number/crypt determined from 20 crypts/mouse and 6 mice/group. Values represent means ± SEM. Statistical analysis was performed using one-way Anova test followed by Bonferroni post-test. ***P* ≤ .01; ****P* ≤ .001.

Figure 6: IEC-specific autophagy deficiency leads to increased colonic cell proliferation in 11G5-infected *Apc$^{Min/+}$* mice.

Apc$^{Min/+}$/Atg16l1$^{\Delta IEC}$ and *Apc$^{Min/+}$* mice were orally administered with PBS or with 10^9 CFU of 11G5 bacteria and sacrificed at day 65 post-administration. **(A)** Representative Western blot analysis of Cyclin D1 level in non-tumoral colonic mucosa and **(B)** quantification of band intensity from N = 7/group for uninfected mice and N = 10/group for 11G5-infected mice. **(C)** *Cyclin D1* mRNA level in the non-tumoral colonic mucosa was quantified by qRT-PCR. Data are means ± SEM (uninfected mice: N = 7/group; *Apc$^{Min/+}$*+11G5: N = 13; *Apc$^{Min/+}$/Atg16l1$^{\Delta IEC}$*+11G5: N = 11) and are representatives of 2 independent experiments. **(D)** Ki67 immunohistochemical staining of colonic mucosa and **(E)** quantification of Ki67-positive cell number/crypt determined from 20 crypts/mouse and 6 mice/group. **(F)** Ki67 immunohistochemical staining of colonic tumors and **(G)** quantification of Ki67$^+$

number/mm^2 of tumor determined from 6 mice/group. Statistical analysis was performed using one-way Anova test followed by Bonferroni post-test. *$P < .05$; **$P \leq .01$; ***$P \leq .001$.

Figure 7: Proposed model for the role of autophagy in colorectal carcinogenesis associated with CoPEC colonization.

In a host predisposed to CRC development, in response to abnormal colonization with CoPEC strains, autophagy is activated to protect colonic epithelium from DNA damage via activating the DNA damage repair, to reduce colonic inflammation and cell proliferation, thus limiting colorectal carcinogenesis. Autophagy dysfunction leads to promoted colorectal carcinogenesis, which is associated with increases in epithelial DNA damage, intestinal inflammation and colonic epithelial cell proliferation.

References

1. Ferlay J, Soerjomataram I, Dikshit R, et al. Cancer incidence and mortality worldwide: Sources, methods and major patterns in GLOBOCAN 2012. Int J Cancer 2015;136:E359–E386.

2. Lucas C, Barnich N, Nguyen HTT. Microbiota, Inflammation and Colorectal Cancer. Int J Mol Sci 2017;18.

3. Moser AR, Pitot HC, Dove WF. A dominant mutation that predisposes to multiple intestinal neoplasia in the mouse. Science 1990;247:322–324.

4. Arvelo F, Sojo F, Cotte C. Biology of colorectal cancer. ecancermedicalscience 2015;9.

5. Li Y, Kundu P, Seow SW, et al. Gut microbiota accelerate tumor growth via c-jun and STAT3 phosphorylation in APC Min/+ mice. Carcinogenesis 2012;33:1231–1238.

6. Zackular JP, Baxter NT, Iverson KD, et al. The Gut Microbiome Modulates Colon Tumorigenesis. mBio 2013;4:e00692-13.

7. **Wong SH, Zhao L**, Zhang X, et al. Gavage of Fecal Samples From Patients With Colorectal Cancer Promotes Intestinal Carcinogenesis in Germ-Free and Conventional Mice. Gastroenterology 2017;153:1621-1633.e6.

8. **Buc E, Dubois D**, Sauvanet P, et al. High prevalence of mucosa-associated *E. coli* producing cyclomodulin and genotoxin in colon cancer. PloS One 2013;8:e56964.

9. Cuevas-Ramos G, Petit CR, Marcq I, et al. *Escherichia coli* induces DNA damage in vivo and triggers genomic instability in mammalian cells. Proc Natl Acad Sci U S A 2010;107:11537–11542.

10. Nougayrède J-P, Homburg S, Taieb F, et al. *Escherichia coli* Induces DNA Double-Strand Breaks in Eukaryotic Cells. Science 2006;313:848–851.

11. **Cougnoux A, Dalmasso G**, Martinez R, et al. Bacterial genotoxin colibactin promotes colon tumour growth by inducing a senescence-associated secretory phenotype. Gut 2014;63:1932–1942.

12. Bonnet M, Buc E, Sauvanet P, et al. Colonization of the Human Gut by *E. coli* and Colorectal Cancer Risk. Clin Cancer Res 2014;20:859–867.

13. Arthur JC, Perez-Chanona E, Mühlbauer M, et al. Intestinal inflammation targets cancer-inducing activity of the microbiota. Science 2012;338:120–123.

14. Tomkovich S, Yang Y, Winglee K, et al. Locoregional effects of microbiota in a preclinical model of colon carcinogenesis. Cancer Res 2017;77:2620–2632.

15. Mizushima N. A brief history of autophagy from cell biology to physiology and disease. Nat Cell Biol 2018;20:521–527.

16. **Singh SS, Vats S**, Chia AY-Q, et al. Dual role of autophagy in hallmarks of cancer. Oncogene 2018;37:1142–1158.

17. Zheng H, Zhang X, Wang X, et al. Autophagy Enhances the Aggressiveness of Human Colorectal Cancer Cells and Their Ability to Adapt to Apoptotic Stimulus. Cancer Biol Med 2012;9:105–110.

18. Jo YK, Kim SC, Park IJ, et al. Increased Expression of ATG10 in Colorectal Cancer Is Associated with Lymphovascular Invasion and Lymph Node Metastasis. PLoS ONE 2012;7.

19. **Yang M, Zhao H**, Guo L, et al. Autophagy-based survival prognosis in human colorectal carcinoma. Oncotarget 2015;6:7084–7103.

20. Raisch J, Buc E, Bonnet M, et al. Colon cancer-associated B2 *Escherichia coli* colonize gut mucosa and promote cell proliferation. World J Gastroenterol WJG 2014;20:6560–6572.

21. Raisch J, Rolhion N, Dubois A, et al. Intracellular colon cancer-associated *Escherichia coli* promote protumoral activities of human macrophages by inducing sustained COX-2 expression. Lab Invest 2015;95:296–307.

22. **Adolph TE, Tomczak MF, Niederreiter L**, et al. Paneth cells as a site of origin for intestinal inflammation. Nature 2013;503:272–276.

23. Umar A, Boland CR, Terdiman JP, et al. Revised Bethesda Guidelines for Hereditary Nonpolyposis Colorectal Cancer (Lynch Syndrome) and Microsatellite Instability. J Natl Cancer Inst 2004;96:261–268.

24. Gagnière J, Bonnin V, Jarrousse A-S, et al. Interactions between microsatellite instability and human gut colonization by *Escherichia coli* in colorectal cancer. Clin Sci 2017;131:471–485.

25. Wang Y, Zhang N, Zhang L, et al. Autophagy Regulates Chromatin Ubiquitination in DNA Damage Response through Elimination of SQSTM1/p62. Mol Cell 2016;63:34–48.

26. Lévy J, Cacheux W, Bara MA, et al. Intestinal inhibition of Atg7 prevents tumour initiation through a microbiome-influenced immune response and suppresses tumour growth. Nat Cell Biol 2015;17:1062–1073.

27. Ma Y, Galluzzi L, Zitvogel L, et al. Autophagy and Cellular Immune Responses. Immunity 2013;39:211–227.

28. **Guo JY, Chen H-Y, Mathew R**, et al. Activated Ras requires autophagy to maintain oxidative metabolism and tumorigenesis. Genes Dev 2011;25:460–470.

29. Li B-X, Li C-Y, Peng R-Q, et al. The expression of beclin 1 is associated with favorable prognosis in stage IIIB colon cancers. Autophagy 2009;5:303–306.

30. Ahn CH, Jeong EG, Lee JW, et al. Expression of beclin-1, an autophagy-related protein, in gastric and colorectal cancers. APMIS 2007;115:1344–1349.

31. Chen Z, Li Y, Zhang C, et al. Downregulation of Beclin1 and Impairment of Autophagy in a Small Population of Colorectal Cancer. Dig Dis Sci 2013;58:2887–2894.

32. **Bretin A, Carrière J**, Dalmasso G, et al. Activation of the EIF2AK4-EIF2A/eIF2α-ATF4 pathway triggers autophagy response to Crohn disease-associated adherent-invasive *Escherichia coli* infection. Autophagy 2016;12:770–783.

33. Lapaquette P, Glasser A-L, Huett A, et al. Crohn's disease-associated adherent-invasive E. coli are selectively favoured by impaired autophagy to replicate intracellularly. Cell Microbiol 2010;12:99–113.

34. Nguyen HTT, Lapaquette P, Bringer M-A, et al. Autophagy and Crohn's Disease. J Innate Immun 2013;5:434–443.

35. Nguyen HTT, Dalmasso G, Müller S, et al. Crohn's Disease–Associated Adherent Invasive *Escherichia coli* Modulate Levels of microRNAs in Intestinal Epithelial Cells to Reduce Autophagy. Gastroenterology 2014;146:508–519.

36. Kostic AD, Chun E, Robertson L, et al. *Fusobacterium nucleatum* potentiates intestinal tumorigenesis and modulates the tumor immune microenvironment. Cell Host Microbe 2013;14:207.

37. **Mima K**, **Nishihara R**, **Qian ZR**, et al. *Fusobacterium nucleatum* in colorectal carcinoma tissue and patient prognosis. Gut 2016;65(12):1973-1980.

38. **Yu T, Guo F**, Yu Y, et al. Fusobacterium nucleatum Promotes Chemoresistance to Colorectal Cancer by Modulating Autophagy. Cell 2017;170:548-563.e16.

39. **Tang B, Wang K**, Jia Y, et al. Fusobacterium nucleatum-Induced Impairment of Autophagic Flux Enhances the Expression of Proinflammatory Cytokines via ROS in Caco-2 Cells. PLoS ONE 2016;11. Available at:

40. **Cohen-Kaplan V**, Ciechanover A, **Livneh I**. p62 at the crossroad of the ubiquitin-proteasome system and autophagy. Oncotarget 2016;7:83833–83834.

41. **Mathew R, Karp C**, Beaudoin B, et al. Autophagy Suppresses Tumorigenesis Through Elimination of p62. Cell 2009;137:1062–1075.

Author names in bold designate shared co-first authorship

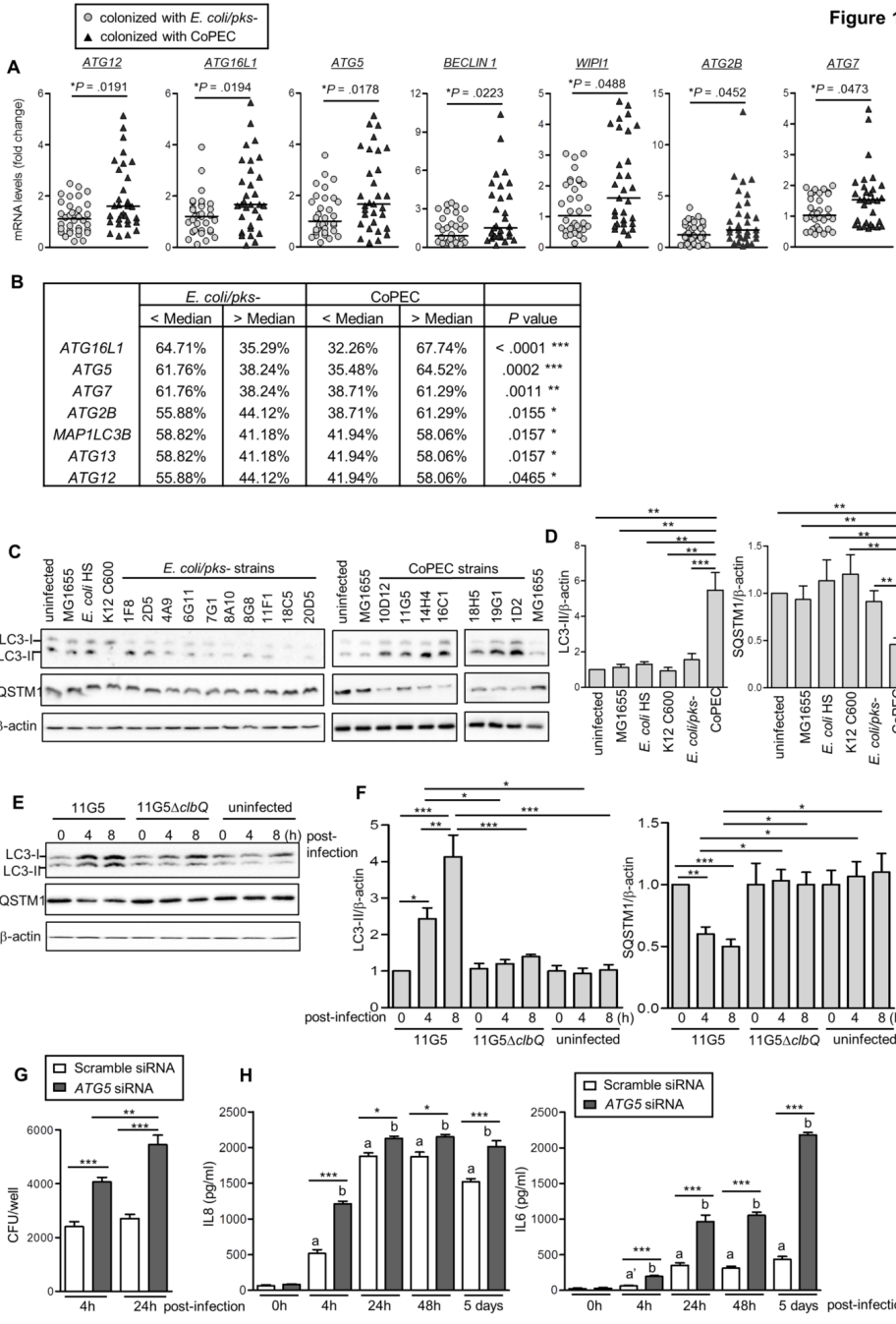

	E. coli/pks-		CoPEC		
	< Median	> Median	< Median	> Median	*P* value
ATG16L1	64.71%	35.29%	32.26%	67.74%	< .0001 ***
ATG5	61.76%	38.24%	35.48%	64.52%	.0002 ***
ATG7	61.76%	38.24%	38.71%	61.29%	.0011 **
ATG2B	55.88%	44.12%	38.71%	61.29%	.0155 *
MAP1LC3B	58.82%	41.18%	41.94%	58.06%	.0157 *
ATG13	58.82%	41.18%	41.94%	58.06%	.0157 *
ATG12	55.88%	44.12%	41.94%	58.06%	.0465 *

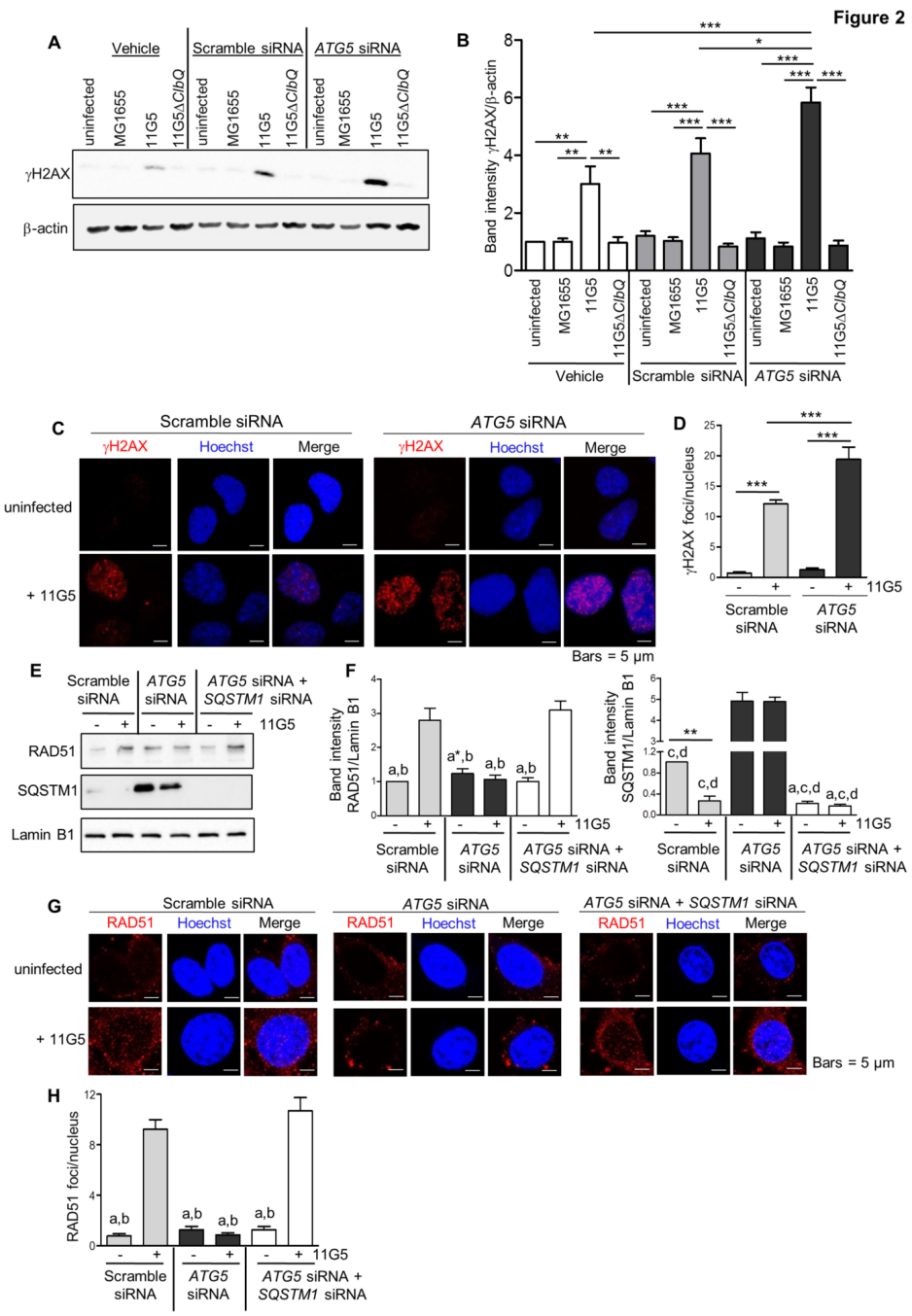
A
Vehicle
Scramble siRNA
ATG5 siRNA
uninfected
MG1655
11G5
11G5ΔClbQ
γH2AX
β-actin
B
Band intensity γH2AX/β-actin
Vehicle
Scramble siRNA
ATG5 siRNA
C
Scramble siRNA
ATG5 siRNA
γH2AX
Hoechst
Merge
uninfected
+ 11G5
Bars = 5 μm
D
γH2AX foci/nucleus
11G5
Scramble siRNA
ATG5 siRNA
E
Scramble siRNA
ATG5 siRNA
ATG5 siRNA + SQSTM1 siRNA
11G5
RAD51
SQSTM1
Lamin B1
F
Band intensity RAD51/Lamin B1
Band intensity SQSTM1/Lamin B1
G
Scramble siRNA
ATG5 siRNA
ATG5 siRNA + SQSTM1 siRNA
RAD51
Hoechst
Merge
uninfected
+ 11G5
Bars = 5 μm
H
RAD51 foci/nucleus
Scramble siRNA
ATG5 siRNA
ATG5 siRNA + SQSTM1 siRNA
11G5

Figure 3

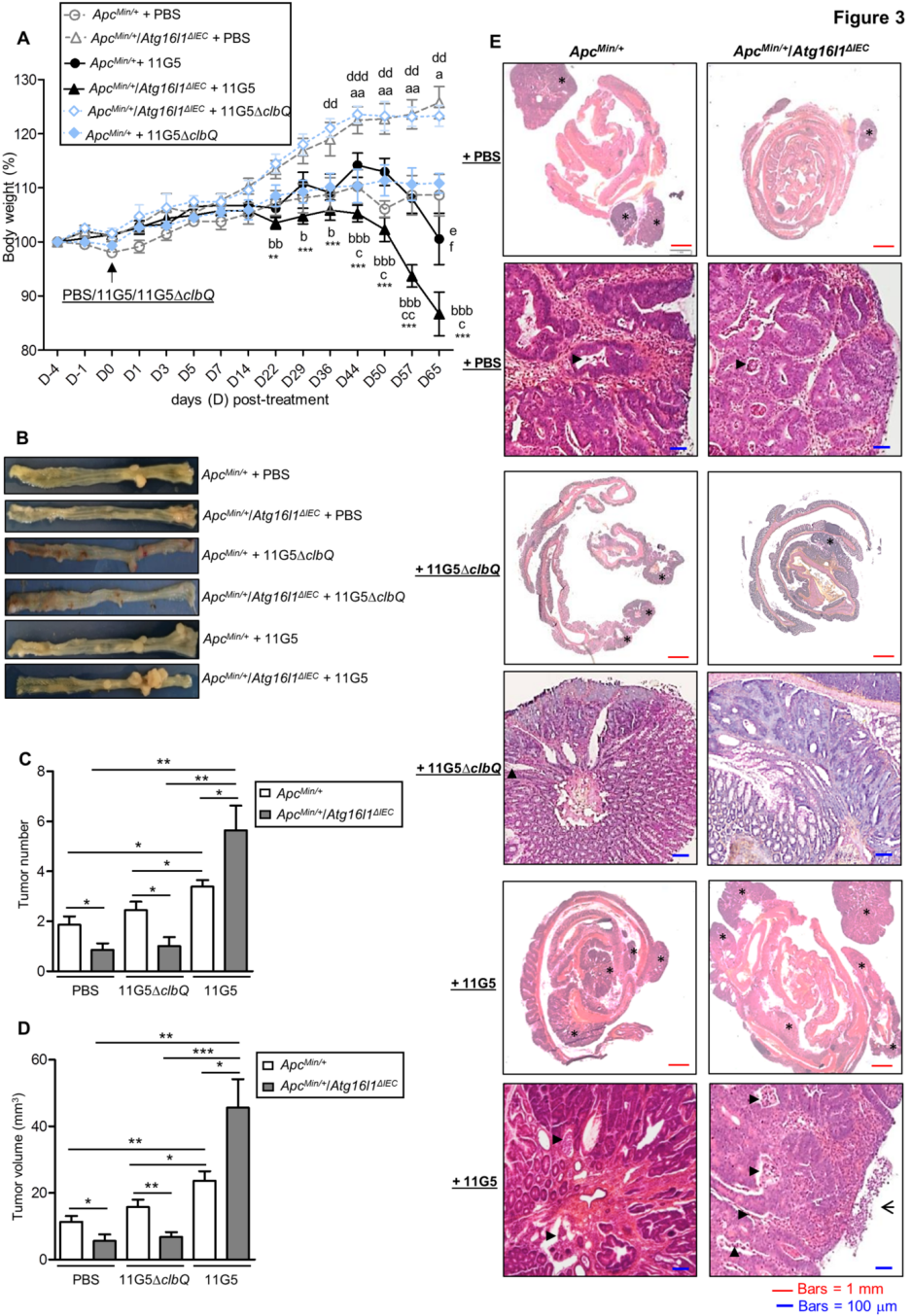
A
ApcMin/+ + PBS
ApcMin/+/Atg16l1ΔIEC + PBS
ApcMin/+ + 11G5
ApcMin/+/Atg16l1ΔIEC + 11G5
ApcMin/+/Atg16l1ΔIEC + 11G5ΔclbQ
ApcMin/+ + 11G5ΔclbQ
Body weight (%)
PBS/11G5/11G5ΔclbQ
days (D) post-treatment
B
ApcMin/+ + PBS
ApcMin/+/Atg16l1ΔIEC + PBS
ApcMin/+ + 11G5ΔclbQ
ApcMin/+/Atg16l1ΔIEC + 11G5ΔclbQ
ApcMin/+ + 11G5
ApcMin/+/Atg16l1ΔIEC + 11G5
C
Tumor number
PBS
11G5ΔclbQ
11G5
D
Tumor volume (mm3)
E
ApcMin/+
ApcMin/+/Atg16l1ΔIEC
+ PBS
+ 11G5ΔclbQ
+ 11G5
Bars = 1 mm
Bars = 100 μm

Figure 4

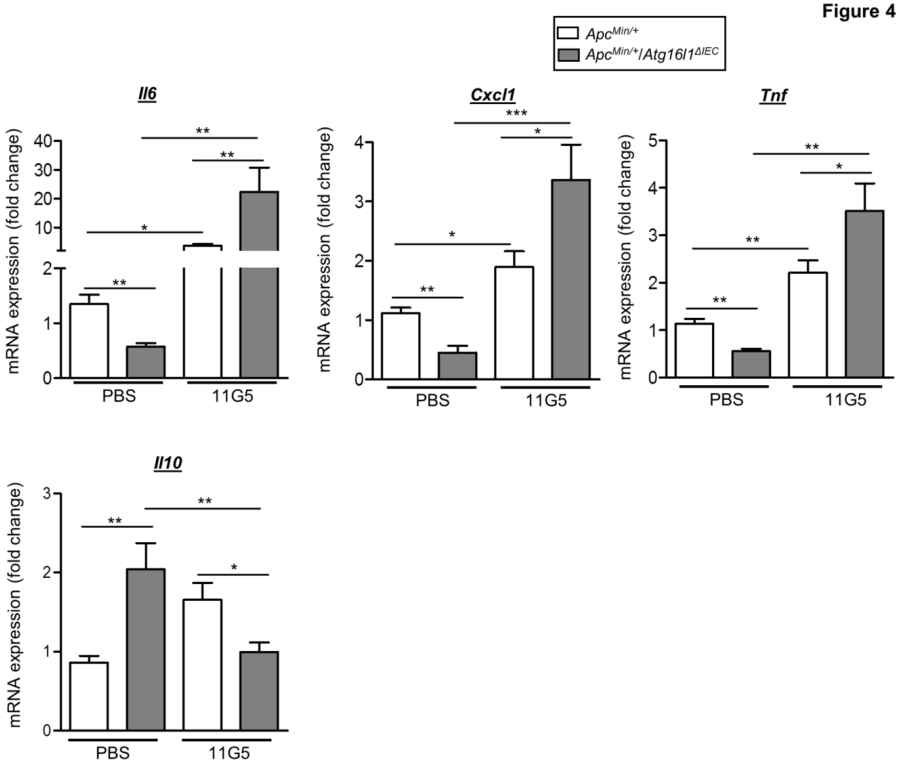
ApcMin/+
ApcMin/+/Atg16l1ΔIEC
Il6
Cxcl1
Tnf
Il10
mRNA expression (fold change)
PBS
11G5

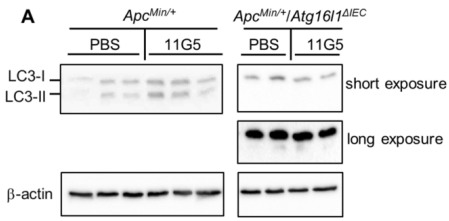
A
ApcMin/+
ApcMin/+/Atg16l1ΔIEC
PBS
11G5
PBS
11G5
LC3-I
LC3-II
short exposure
long exposure
β-actin

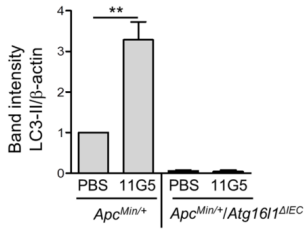
B
Band intensity
LC3-II/β-actin
**
PBS
11G5
PBS
11G5
ApcMin/+
ApcMin/+/Atg16l1ΔIEC

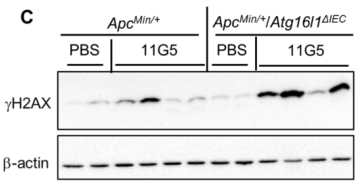
C
ApcMin/+
ApcMin/+/Atg16l1ΔIEC
PBS
11G5
PBS
11G5
γH2AX
β-actin

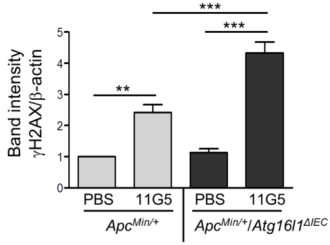
D
Band intensity
γH2AX/β-actin
***
***
**
PBS
11G5
PBS
11G5
ApcMin/+
ApcMin/+/Atg16l1ΔIEC

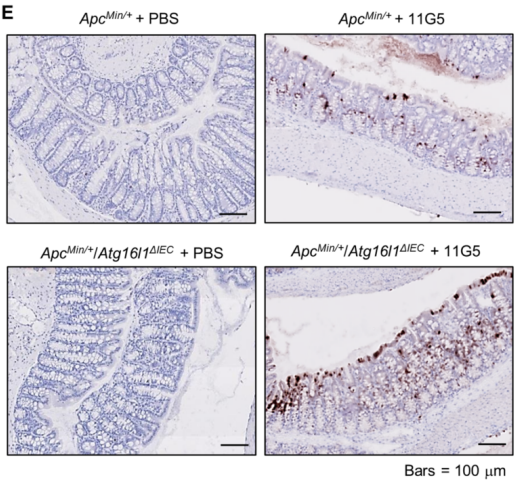
E
ApcMin/+ + PBS
ApcMin/+ + 11G5
ApcMin/+/Atg16l1ΔIEC + PBS
ApcMin/+/Atg16l1ΔIEC + 11G5
Bars = 100 μm

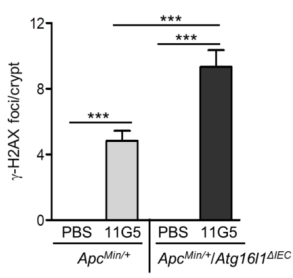
F
γ-H2AX foci/crypt
***
***
***
PBS
11G5
PBS
11G5
ApcMin/+
ApcMin/+/Atg16l1ΔIEC

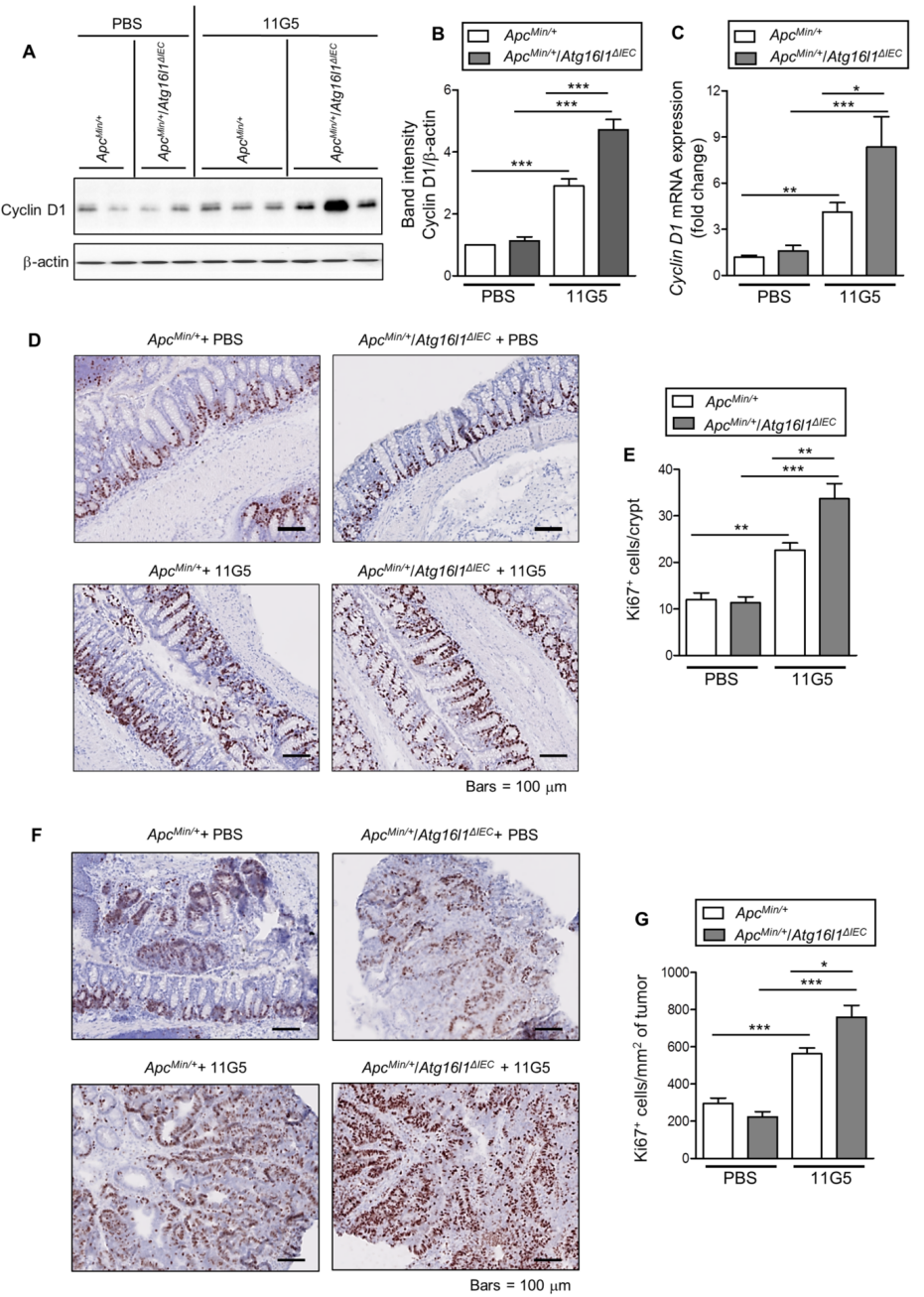
A
PBS
11G5
ApcMin/+
ApcMin/+/Atg16l1ΔIEC
Cyclin D1
β-actin
B
Band intensity Cyclin D1/β-actin
PBS
11G5
C
Cyclin D1 mRNA expression (fold change)
D
ApcMin/+ + PBS
ApcMin/+/Atg16l1ΔIEC + PBS
ApcMin/+ + 11G5
ApcMin/+/Atg16l1ΔIEC + 11G5
Bars = 100 μm
E
Ki67+ cells/crypt
F
ApcMin/+ + PBS
ApcMin/+/Atg16l1ΔIEC + PBS
ApcMin/+ + 11G5
ApcMin/+/Atg16l1ΔIEC + 11G5
Bars = 100 μm
G
Ki67+ cells/mm2 of tumor

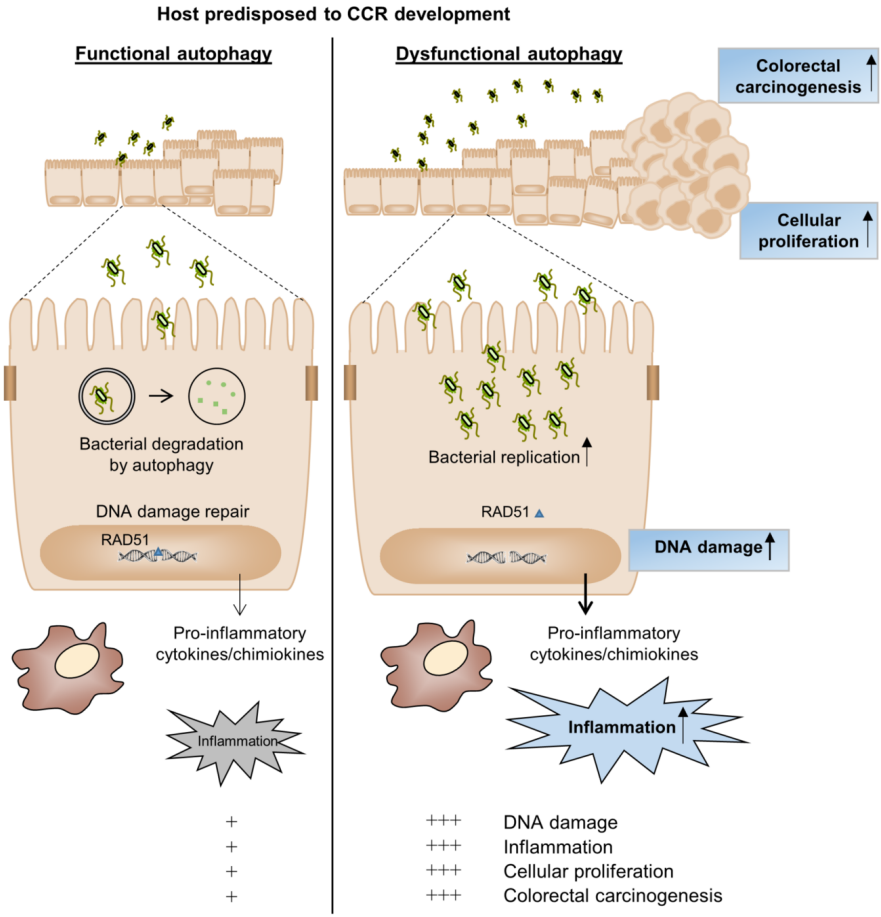
Host predisposed to CCR development
Functional autophagy
Dysfunctional autophagy
Colorectal carcinogenesis
Cellular proliferation
Bacterial degradation by autophagy
DNA damage repair
RAD51
Bacterial replication
RAD51
DNA damage
Pro-inflammatory cytokines/chimiokines
Pro-inflammatory cytokines/chimiokines
Inflammation
Inflammation
+
+
+
+
+++ DNA damage
+++ Inflammation
+++ Cellular proliferation
+++ Colorectal carcinogenesis

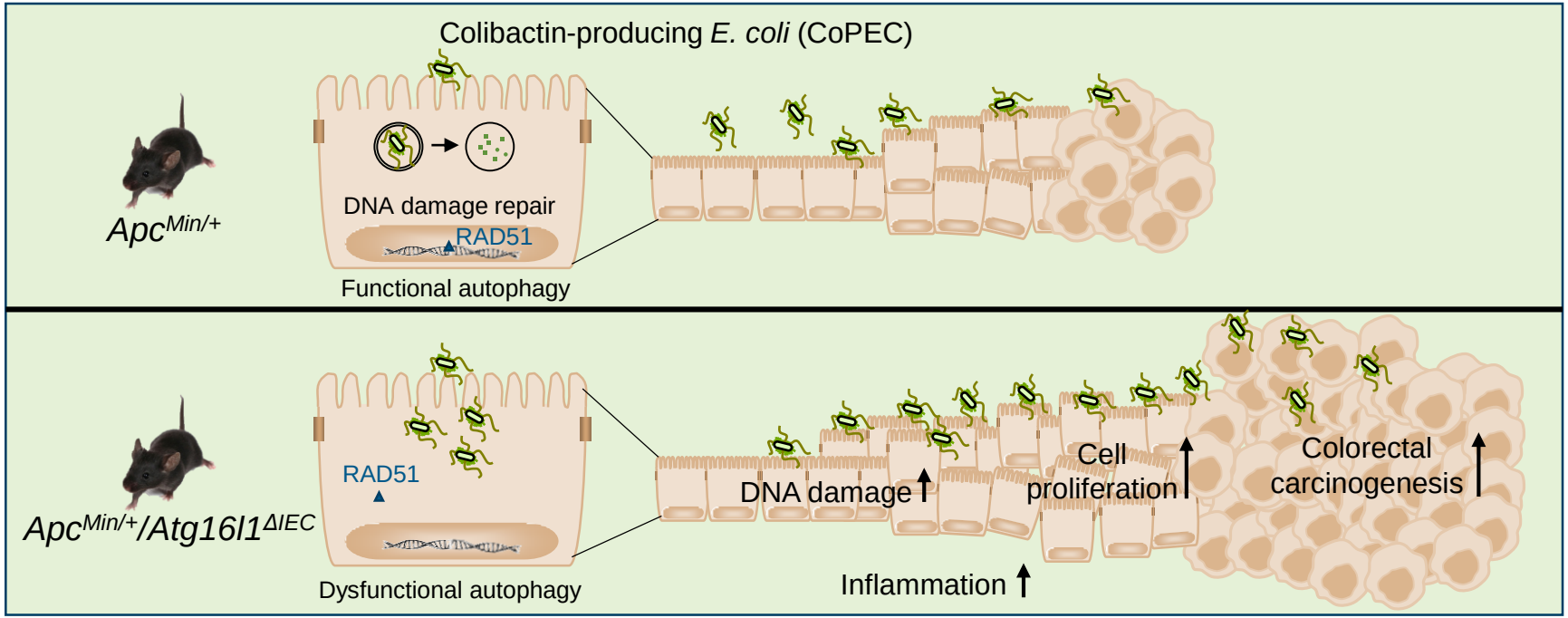

Gastroenterology